Journal of Nuclear Materials 386–388 (2009) 675–677

Contents lists available at ScienceDirect

Journal of Nuclear Materials

journal homepage: www.elsevier.com/locate/jnucmat

Calculation of dissolution/deposition rates in flowing eutectic Pb–17Li with the MATLIM code

H. Steiner *, W. Krauss, J. Konys

Forschungszentrum Karlsruhe, Institut für Materialforschung III, Hermann-von-Helmholtz-Platz 1, D-76344 Eggenstein-Leopoldshafen, Germany

A B S T R A C T

It is generally accepted that corrosion of steel components in flowing liquid Pb–17Li is ruled by dissolution/deposition processes. A simple method has been devised to calculate the mass transfer in liquid metal loops. It is based on the use of mass transfer coefficients which determine the mass flux from the wall into the fluid and vice versa. These coefficients depend on a characteristic dimensionless thermo-hydraulic number, namely the Sherwood number, which itself depends under forced convection flow conditions on the Reynolds number and the Schmidt number. This is supplemented by the application of differential equations for dissolved steel components. The dissolution and deposition rates determine then the evolution of the flow channel geometry along the loop and the flow velocity. The newly developed code MATLIM can routinely deal with multi-modular liquid metal loops. Thus, calculations have been done for the PICOLO loop based on iron solubility and diffusivity correlations of Feuerstein et al.

1. Introduction

Pb–17Li alloy is considered as a coolant and breeding medium in future fusion reactors. One major problem in non-isothermal liquid metal systems lies in the corrosion of their structural materials, consisting mainly of martensitic and austenitic stainless steels. It is generally accepted that corrosion of steel components in flowing liquid Pb–17Li is ruled by dissolution processes. Although Pb–17Li loops are operated with low oxygen concentrations preventing the formation of new oxide phases, we must foresee the possibility of oxide scales or other protective layers on structural components.

The locations of dissolution and deposition are mainly determined by the temperature dependence of the solubility of iron. This means that we have dissolution in the hot parts of the system and deposition in the cold parts, irrespective of the nature of the dissolution process, whether it is exothermic or endothermic.

We have developed a simple model, which calculates the mass transfer and the geometrical changes of structural components in liquid metal loops. This model was implemented in the computer code MATLIM.

2. Theoretical background

The mass flux of the solute i from the channel wall into the bulk of the fluid is calculated in MATLIM [1,2] with the help of the following equation:

$$j_i = K_i^{fl} \cdot (c_i^w - c_i^b), \tag{1}$$

K_i^{fl} is the mass transfer coefficient for the solute i, c_i^w the concentration of the solute i at the wall and c_i^b is the concentration in the bulk of the fluid.

The mass transfer coefficient K_i^{fl} is determined by the Sherwood number Sh in the following way [3]:

$$K_i^{fl} = \frac{D_i}{d_{\mathrm{hyd}}} \cdot Sh, \tag{2}$$

d_{hyd} is the hydraulic diameter and D_i the diffusion coefficient in the liquid metal.

The calculation of the solute concentration in the bulk of the fluid c_i^b along the whole loop is done with the help of the mass conservation law:

$$\frac{\partial c_i^b(t,x)}{\partial t} + u_{fl} \cdot \frac{\partial c_i^b(t,x)}{\partial x} = \frac{U_{\mathrm{ch}}}{A_{\mathrm{ch}}} \cdot j_i(t,x), \tag{3}$$

U_{ch} is the circumference of the flow channel, A_{ch} the cross section of the flow channel, j_i the mass flux and u_{fl} the flow velocity in the coolant channel. The flow velocity u_{fl} is calculated from the measured mass flow rate. For the time being we are only considering quasi steady-state conditions. Thus, the first term in Eq. (3) is not

* Corresponding author.
E-mail address: helmut.steiner@imf.fzk.de (H. Steiner).

0022-3115/$ - see front matter © 2009 Elsevier B.V. All rights reserved.
doi:10.1016/j.jnucmat.2008.12.267

taken into account. Eq. (3) is solved with the help of an iterative procedure starting with pre-defined initial values for c_i^b.

There are mainly three different types of physical properties and parameters, which determine material behavior in a liquid metal system. The first group concerns the thermo-hydraulic data of the system like the flow velocity and the hydraulic diameter but also the temperature distribution along the system. The second group concerns material data like viscosity of the liquid metal, diffusivity and solubility of the solutes. The third group encompasses properties of the wall materials itself.

3. Dissolution and deposition rates and evolution of the channel inner wall radius

We have now all the necessary elements for the calculation of the dissolution and the deposition rates, one of the main aims of this work. We are mainly concerned with stainless steel components.

As iron is the major steel constituent it is assumed that this element determines dissolution and deposition rates b_{me}:

$$b_{me} = -j_{Fe} \cdot \frac{1}{\rho_{ss} \cdot f_{Fe}}, \tag{4}$$

ρ_{ss} = specific mass density of stainless steel f_{Fe} = iron mass fraction in stainless steel.

The change of the inner channel radius in a time interval Δt is given by:

$$\Delta r_i^{ch} = -b_{me} \cdot \Delta t. \tag{5}$$

4. Correlations for the mass transfer coefficient, for the solubility and diffusivity

There are a number of correlations for the mass transfer coefficient obtained under fully developed turbulent pipe flow. Our main assumption is that they can also be applied for liquid metal loops. Three of these correlations were investigated and discussed in Ref. [3]. These are the correlation of Berger and Hau [4], that of Silverman [5], and that of Harriott and Hamilton [6]. All these three correlations give similar values for the mass transfer coefficient. It is therefore sufficient for us to use only one of them, namely that of Silverman [5]:

$$K_{Silv} = 0.0177 \cdot u_{fl}^{0.875} \cdot D_{Fe}^{0.704} / (d_{hyd}^{0.125} \cdot \upsilon_{fl}^{0.567}). \tag{6}$$

Values of the iron solubility and diffusivity are very important for the model used in MATLIM, and great care must be applied in selecting appropriate correlations. Correlations for the iron solubility in Pb–17Li were given in Refs. [3,7–10]: The values differ by orders of magnitude. The data obtained by Feuerstein et al. [10] for alpha-Iron are compatible with values of the iron diffusivity being in a reasonable range (10^{-10}–10^{-9} m^2/s) and deemed us the most trustworthy ones.

The following correlation has been given in [10]:

$$c_{Fe}^s(T) = e^{4.94-4992/T} \quad \text{in wppm}. \tag{7}$$

It is evident from the work in Ref. [10] that the iron solubility over stainless steels is somewhat different from that over alpha-Iron. Thus, there must be some variation with the steel composition. It should be noted that the dissolution of alloys and compounds in Pb–17Li is not well-understood.

The authors in Ref. [10] have deduced the following correlation for the iron diffusivity from the dissolution rates in crucibles by applying a simple model:

$$D_{Fe}(T) = e^{-19.64-2844/T} \quad \text{in m}^2/\text{s}. \tag{8}$$

5. Results of calculations for the PICOLO loop with the MATLIM code

A description of the PICOLO loop can be found in Ref. [11] and is therefore not repeated in this report. The loop has recently been upgraded to a maximum temperature of about 550 °C and the main aim of the calculations with the MATLIM code was to estimate the effect of the temperature increase on the dissolution rates. It should be noted that in low temperature case (480 °C) the MATLIM code has calculated a dissolution rate of about 80 μm/y for a flow velocity of 22 cm/s [12].

The code MATLIM provides a 1-D simulation of the multi-modular PICOLO loop, with Fig. 1 showing the axial profiles of the hydraulic diameter and of the calculated flow velocity along the whole loop. The flow velocity has its highest value along the test section loaded with the test specimens (22 cm/s) and is lowest inside the magnetic trap (1 cm/s).

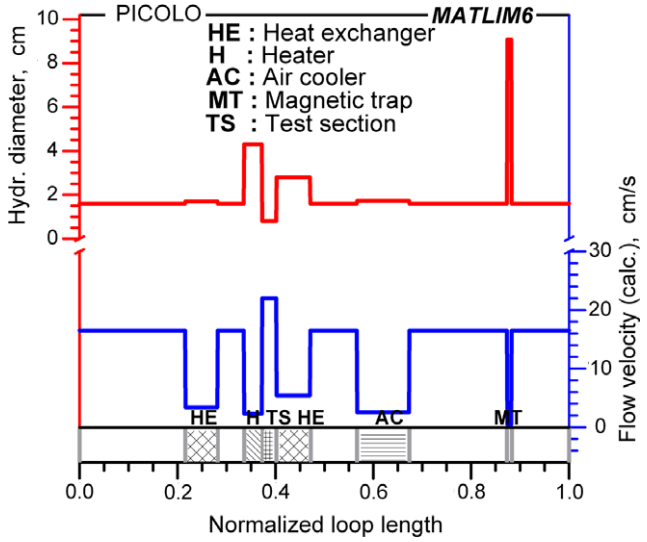

Fig. 1. Axial distributions of the flow velocity and the hydraulic diameter in the PICOLO loop.

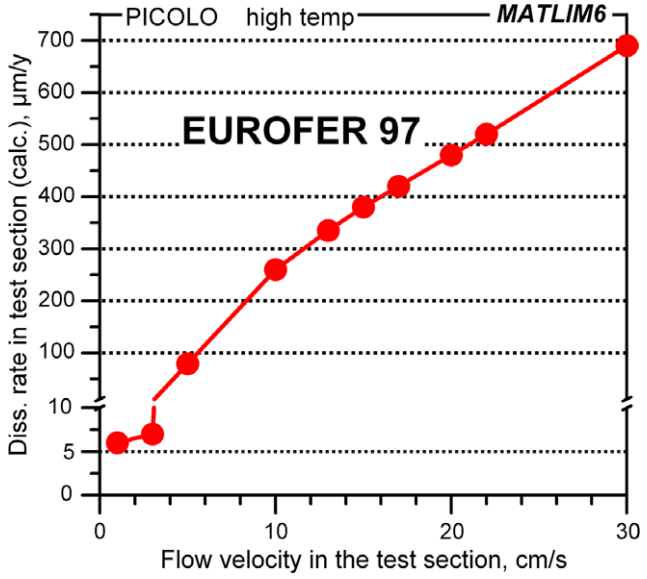

Fig. 2. Dissolution rate in the test section of the PICOLO loop versus flow velocity.

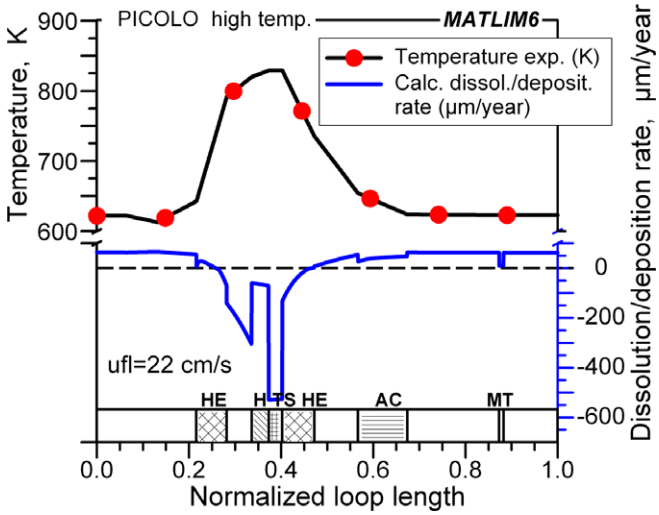

Fig. 3. Axial distributions of temperature and dissolution/deposition rates in the loop (high temp. case).

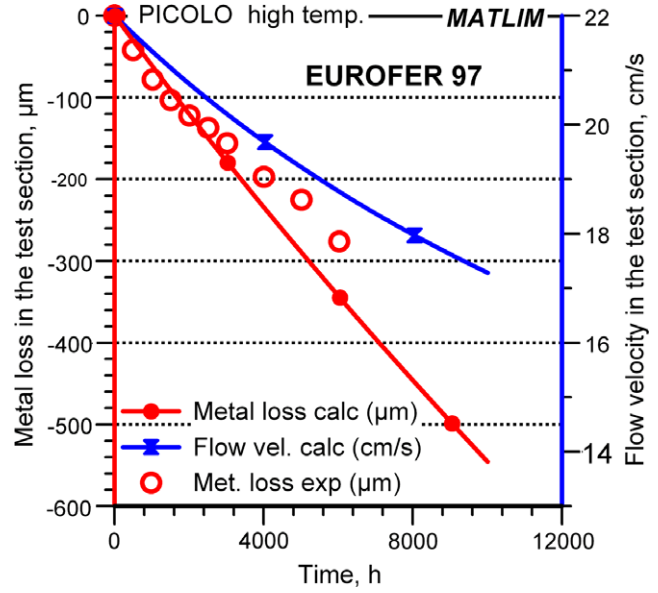

Fig. 4. Dissolution layer and flow velocity in the test section of the PICOLO loop versus time.

The design parameter of greatest interest concerns the flow velocity in the test section. Fig. 2 shows for the high temperature case how the dissolution rate in the test section evolves with increasing flow velocity. For a value less equal 3 cm/s we are in the laminar flow regime, between 3 and 10 cm/s in the transition regime, and above 10 cm/s in the fully turbulent flow regime. It should be noted that in the fully developed laminar flow regime the Sherwood number is independent of the flow velocity. For the laminar flow regime the code predicts very low (a few μm/y) but non-zero dissolution rates.

Due to the dissolution/deposition effects the flow channel along the loop changes its size during the operation. This effect is most important in the test section where dissolution leads to an increase of the cross section and therefore to a decrease of the flow velocity with the effect considerably enhanced for the high temperature condition. The test campaign for EUROFER started with a flow velocity in the test section of 22 cm/s. A value of 20 cm/s is representative for test durations of 5000 h and a value of 17 cm/s after 10 000 h.

For a value of the flow velocity in the test section of 22 cm/s the dissolution/deposition rates along the loop are shown in Fig. 3. It should be noted that due to the convention used in the MATLIM code negative values stand for dissolution and positive values for deposition. The maximum dissolution rates are to be found in the loaded test section. The axial profiles of the dissolution/deposition rates are rather perturbed, a consequence of the hydraulic properties of the different components.

Due to corrosion of the test specimens and corrosion of the channel wall the flow velocity in the test section decreases with time as the channel cross section increases and as the mass flow rate is kept constant. Fig. 4 shows the evolution of the flow velocity and the dissolution layer in the test section as calculated by MATLIM6 together with experimental values. The increase of the dissolution layer is not strictly linear with time as the flow velocity decreases from 22 cm/s to about 17 cm/s within test duration of about 11 000 h.

6. Conclusion

A kinetic model for the calculation of mass transfer in liquid metal systems under forced convection flow conditions has been developed. It is based on the use of the relevant characteristic thermo-hydraulic numbers, which determine the mass flux from the wall into the fluid. This is supplemented by the application of the mass conservation law to calculate the conditions in the bulk of the fluid. The dissolution/deposition rates determine then the geometrical changes of the structural components. For metallic surfaces the dissolution rates can be considerable. In this case a lot of experimental data are available. If oxide scales are present the dissolution rates should be very much smaller.

In a first round of calculations for the PICOLO loop we have started to validate the newly developed code MATLIM. For this we have used correlations for the iron solubility and iron diffusivity provided by Feuerstein et al. These correlations yield reasonable results for the dissolution rates. With the code MATLIM a simple and flexible tool for the calculation of mass transfer and geometrical changes in liquid metal loops is now available at FZK.

Acknowledgement

This work, supported by the European Communities under the contract of Association between EURATOM and Forschungszentrum Karlsruhe, was carried out within the framework of the European Fusion Development Agreement. The views and opinions expressed herein do not necessarily reflect those of the European Commission.

References

[1] T. Malkow, H. Steiner, H. Muscher, J. Konys, J. Nucl. Mater. 335 (2004) 199.
[2] H. Steiner, J. Konys, J. Nucl. Mater. 348 (2006) 18.
[3] F. Balbaud-Celerier, F. Barbier, J. Nucl. Mater. 289 (2001) 227.
[4] F.P. Berger, K. Hau, Int. J. Heat Mass Transfer 20 (1977) 1185.
[5] D.C. Silverman, Corrosion 55 (1999) 1115.
[6] P. Harriott, R.M. Hamilton, Chem. Eng. Sci. 20 (1965) 1073.
[7] M.G. Barker, V. Coen, H. Kolbe, J.A. Lees, L. Orecchia, T. Sample, J. Nucl. Mater. 155–157 (1988) 732.
[8] M.G. Barker, T. Sample, Fus. Eng. Des. 14 (1991) 219.
[9] H.U. Borgstedt, H. Feuerstein, J. Nucl. Mater. 191–194 (1992) 988.
[10] H. Feuerstein, H. Gräbner, J. Oschinski, J. Beyer, S. Horn, L. Hörner, K. Santo, FZKA 5596 (1995).
[11] H. Glasbrenner, J. Konys, Z. Voss, J. Nucl. Mater. 281 (2000) 225.
[12] W. Krauss, J. Konys, H. Steiner, J. Novotny, Z. Voss, O. Wedemeyer, FZKA report 7295 (2007).